Available online at www.sciencedirect.com
ScienceDirect
Comput. Methods Appl. Mech. Engrg. 283 (2015) 956–970
Computer methods in applied mechanics and engineering
www.elsevier.com/locate/cma

Nonlinear dynamic response topology optimization using the equivalent static loads method

Hyun-Ah Lee[a], Gyung-Jin Park[b,*]

[a] Research Institute of Engineering and Technology, Hanyang University, Ansan City, Gyeonggi-do, 426-791, Republic of Korea
[b] Department of Mechanical Engineering, Hanyang University, Ansan City, Gyeonggi-do, 426-791, Republic of Korea

Received 5 December 2013; received in revised form 18 August 2014; accepted 16 October 2014
Available online 27 October 2014

Abstract

A novel method for nonlinear dynamic response topology optimization is proposed using the equivalent static loads (ESLs) method. The ESLs are the loads that generate the same response field of linear static analysis as that of nonlinear dynamic analysis at each time step. In the proposed procedure, nonlinear dynamic analysis is performed, ESLs are made and linear static topology optimization is carried out with the ESLs. The process cyclically proceeds until the convergence criterion, which is specifically defined for this problem, is satisfied. Since the density method for topology optimization is utilized, the low-density finite elements can cause mesh distortion in nonlinear dynamic analysis. Transformation variables are introduced for a new update method for the incorporating process of the topology results into nonlinear dynamic analysis. Also, a new objective function is proposed to minimize the peaks of the time dependent transient responses. A couple of standard problems and a practical problem are solved to validate the proposed method.

Keywords: Nonlinear dynamic response topology optimization; Structural optimization; Equivalent static loads

1. Introduction

Topology optimization finds the optimal layout of a structure by determining the distribution of the material in the design region [1]. There are two methods for topology optimization: the homogenization method [2] and the density method [3]. Commercial software systems for topology optimization such as NASTRAN [4], GENESIS [5] and OptiStruct [6] adopt the density method and the density method is employed in this research. Mostly, topology optimization has been carried out with linear finite element (FE) analysis. However, structural problems have various nonlinearities under dynamic loads in the real world. Thus these nonlinearities and dynamic characteristics should be accommodated in topology optimization. The nonlinearities are related to geometry, material, and contact. FE analysis techniques regarding nonlinear dynamic behavior have been developed very well [7,8]. Performing structural optimization using nonlinear analysis is quite expensive due to heavy computational time for function and sensitivity

* Corresponding author. Tel.: +82 31 400 5246; fax: +82 31 407 0755.
E-mail address: gjpark@hanyang.ac.kr (G.-J. Park).

http://dx.doi.org/10.1016/j.cma.2014.10.015
0045-7825/

analyses. Moreover, including dynamic characteristics in optimization is even more difficult because transient behavior in the time domain should be considered. Thus it is extremely complicated to consider nonlinearities and dynamic responses simultaneously in topology optimization.

Other than the cost, there are two representative obstacles in nonlinear dynamic response topology optimization. First, topology optimization in the time domain frequently uses the summation of the compliance in the entire time range as the objective function [9,10]. In this case, although the overall compliance is minimized, the compliance at some local specific time points can be rapidly increased. Therefore, the values of the compliance at specific time points should be considered when defining the objective function. Another obstacle is the mesh distortion problem when nonlinear analysis is utilized in topology optimization. Elements with low-density may appear in topology optimization based on the element density. Low-density elements can cause excessive mesh distortion in nonlinear analysis, and deteriorate the convergence of the topology optimization process. The first problem is due to the dynamic behavior and the second one is from nonlinearity.

Many researches have been developed for topology optimization with dynamic or nonlinear characteristics. Recently, nonlinear dynamic response topology optimization is performed for crashworthiness optimization by some researchers. Internal energy [11,12] or internal energy density [13] is used as the objective function for topology optimization of the structure in a crash situation. In these researches, optimization is conducted for the responses at the final time steps. However, the general response of a structure with nonlinear dynamic behavior fluctuates during the time duration. Therefore, the values of the responses in the entire time range should be included in the objective or constraint functions. Recently, some researches have been carried out to overcome the mesh distortion problem by proposing new types of elements or convergence relaxation method [14–18]. The methods can control the mesh distortion problem quite effectively. Although the ideas are quite good, the process may not converge with these methods, or many function calculations are required in nonlinear response topology optimization.

A new topology optimization strategy for the dynamic and nonlinear characteristics is proposed by using the equivalent static loads method for nonlinear static response structural optimization (ESLSO). The equivalent static loads (ESLs) are the loads that generate the same response field of linear static analysis as that of nonlinear dynamic analysis at each time step. A nonlinear dynamic response optimization problem is converted into sequential use of linear static response optimization with ESLs. It is noted that optimization is carried out using linear analysis. The idea of ESLSO was initially proposed for linear dynamic response size and shape optimization by Choi and Park in 2002 [19]. ESLSO was expanded for nonlinear static response [20] and nonlinear dynamic response [21] size and shape optimization. Topology optimization for linear dynamic system using ESLSO was proposed by Jang et al. [10,22]. Nonlinear static topology optimization strategy using ESLSO is researched by Lee et al. [18].

ESLSO is expanded for nonlinear dynamic response topology optimization by using a newly defined flow and the two previously mentioned problems are overcome. A newly defined objective function, which is to minimize the peaks of the compliance in the time domain, is utilized to prevent the phenomenon that the compliances of some specific times are abnormally increased. In ESLSO, mesh distortion does not occur during the optimization process because linear analysis is utilized in topology optimization. However, we can have mesh distortion during nonlinear analysis where the results of optimization are incorporated. A technique to prevent mesh distortion is utilized by introduction of the transformation variables and a new updating scheme of design variables for nonlinear dynamic analysis.

Two examples are solved to validate the proposed method. First, topology optimization of a plate fixed along the two ends is carried out by adopting a newly defined objective. The second example is a practical problem with a crash box for crashworthiness design. The objective function is to maximize the maximum absorbed energy of the structure in the time domain. Nonlinear dynamic or crash analysis is carried out by ABAQUS [23] or LS-DYNA [24], GENESIS [5] is utilized for linear static response topology optimization and NASTRAN DMAP (direct matrix abstraction program) [25] is used for calculating the ESLs. A program to interface the commercial systems and the automatic process of the proposed method is developed by the C++ language [26].

2. Topology optimization issues with nonlinear dynamic characteristics

As mentioned earlier, the density method is employed in this study. Topology optimization methods for linear static characteristics have been successful in many applications while topology optimization with nonlinear dynamic characteristics has some issues. These issues are described in this section.

2.1. Definition of the objective function

In topology optimization, various responses have been used as the objective function and constraints: compliance, displacement, stress, etc. The purpose of topology optimization is often maximizing the stiffness of the structure that is used in this paper. Maximizing stiffness is equivalent to minimizing the compliance of the structure. Thus, the objective function is to minimize the compliance of the structure with a specific volume. The general formulation in the density method for linear static response topology optimization is as follows:

$$\begin{aligned}
&\text{Find} && \mathbf{b} \in R^n && \text{(1a)}\\
&\text{to minimize} && \mathbf{f}^{\mathrm{T}}\mathbf{z} && \text{(1b)}\\
&\text{subject to} && \mathbf{K}\mathbf{z} - \mathbf{f} = 0 && \text{(1c)}\\
& && \mathbf{v}^{\mathrm{T}}\mathbf{b} \leq V && \text{(1d)}\\
& && 0.0 < b_{\min} < b_i < 1.0: \quad i = 1, \ldots, n && \text{(1e)}
\end{aligned}$$

where the design variable vector $\mathbf{b}$ is the artificial density of finite elements, n is the number of elements (design variables), $\mathbf{f}^{\mathrm{T}}\mathbf{z}$ is the compliance, $\mathbf{K}$ is the stiffness matrix, $\mathbf{z}$ is the linear static displacement vector, $\mathbf{f}$ is the external load vector and $\mathbf{v}$ is the volume vector of the finite elements. V is the specific volume of the structure defined by the designer and is called volume fraction. b_i is the ith design variable and $b_{\min}$ is the lower bound of the design variable.

When nonlinear dynamic response topology optimization is performed, the compliance is evaluated in the time domain by the following equation:

$$\boldsymbol{\sigma}_u(\mathbf{z})^{\mathrm{T}}\,\boldsymbol{\varepsilon}_u(\mathbf{z}): \quad u = 1, \ldots, l \tag{2}$$

where $\boldsymbol{\sigma}_u(\mathbf{z})$ is the 2nd Piola–Kirchhoff stress tensor at the uth time step, $\boldsymbol{\varepsilon}_u(\mathbf{z})$ is the Green–Lagrange strain tensor at the uth time step and l is the total number of time steps in the time domain. Thus, the summation of the compliance in the entire time domain is utilized as the following objective function:

$$\sum_{u=1}^{l} w_u \left(\boldsymbol{\sigma}_u(\mathbf{z})^{\mathrm{T}}\,\boldsymbol{\varepsilon}_u(\mathbf{z})\right): \quad u = 1, \ldots, l \tag{3}$$

where w_u is the weighting factor. Some researchers used the above objective function in linear dynamic response topology optimization [9,10]. In this case, the summed compliance can be reduced in the optimized model, however, the compliance at some particular time steps can be rapidly increased, and the structure can have a large deformation at those time steps. In other words, the compliance at each time step may not be fully controlled.

To overcome the above difficulty, a new objective function is proposed for nonlinear dynamic response topology optimization. When the compliance is evaluated in the time domain, there are peaks on the compliance profile. The new objective function is defined by the weighted summation of the compliances near the peaks as follows:

$$\sum_{u=1}^{p} w_u \left(\boldsymbol{\sigma}_u(\mathbf{z})^{\mathrm{T}}\,\boldsymbol{\varepsilon}_u(\mathbf{z})\right): \quad u = 1, \ldots, p \tag{4}$$

where p is the number of time steps near the peaks when the total number of time steps is l. Thus, p is always smaller than l. In this case, the average of the compliance of the optimized model might be large. However, the compliance at the peak point will be decreased and the compliance is evenly distributed in the entire time range [22]. If we select only the largest peak point in Eq. (4), the compliance at the other points can be increased during the optimization iteration. Also, if only the peak points are included in Eq. (4), the points near the peaks can be increased. Therefore, the values of multiple time steps near the peaks are included in the objective function of Eq. (4). This technique has been used in size and shape optimizations using linear dynamic analysis [27]. During the optimization process, the number of peaks can be changed. Then p is changed at each optimization cycle.

Eqs. (2)–(4) show the compliance for nonlinear dynamic response topology optimization. As mentioned earlier, nonlinear dynamic response topology optimization is carried out by using nonlinear dynamic analysis and linear static topology optimization. p in Eq. (4) is determined from nonlinear dynamic analysis. Linear static topology optimization

is conducted with p and the following equation as the objective function:

$$\sum_{u=1}^{p} w_u \left(\mathbf{f}_u^{\mathrm{T}} \mathbf{z}_u\right): \quad u = 1, \ldots, p \tag{5}$$

where $\mathbf{f}_u$ is the magnitude of the load vector, $\mathbf{z}_u$ is the displacement vector at the uth time step and $\mathbf{f}_u^{\mathrm{T}}\mathbf{z}_u$ is the linear compliance at the uth time step. This will be explained in Section 3.

2.2. Mesh distortion problem

As mentioned earlier, mesh distortion occurs due to low-density elements in nonlinear analysis. In the conventional element density approach, some elements can have a value of the lower bound during or after the topology optimization process. When nonlinear analysis is performed during nonlinear topology optimization, the tangent stiffness matrices of the low-density elements may be zero or negative. In this case, the low-density elements undergo extreme mesh distortion and have negative volumes. This mesh distortion phenomenon leads to many Newton–Raphson iterations or divergence. Some methods were proposed to overcome the mesh distortion problem [14–17].

In ESLSO, optimization is carried out by using linear analysis and the design variables are updated by the optimization results. The updated results are utilized in nonlinear dynamic analysis. Thus, mesh distortion does not occur during the topology optimization process due to the characteristics of linear analysis. If a design variable has a lower bound after topology optimization, it is replaced by zero. Then the corresponding element is eliminated in nonlinear analysis and the mesh distortion problem is avoided in nonlinear analysis.

The above issues are solved in the newly proposed method and explained theoretically in detail in the next section. The proposed theory will be validated via some examples in Section 4.

3. Proposed method for nonlinear dynamic response topology optimization

As mentioned earlier, the ESLs are defined as the linear static loads that generate the same displacement fields in linear static analysis as those of nonlinear dynamic analysis at an arbitrary time [21]. The ESLs are calculated by the results of nonlinear dynamic analysis. Dynamic characteristics (inertia effects) are included in the ESLs generated from the results of nonlinear dynamic analysis in ESLSO. When we design structures to improve the dynamic characteristics, we can use some positive methods such as anti-resonance or change of supports. If we do not use such positive methods, we may say that we are using a quasi-static method. However, such positive methods cannot be used in optimization at the present time. That is, optimization cannot create anti-resonance or change the supports. It only changes the structural dimensions. In the optimization community it is called dynamic response optimization. Many of the conventional methods [4,9,27] and the Refs. [19,21,22] performed dynamic response optimization in this manner. Therefore, topology optimization using the ESLs is called nonlinear dynamic response topology optimization in this paper.

The original ESLSO is modified for nonlinear dynamic response topology optimization. The newly proposed ESLSO overcomes the issues described in Section 2.

3.1. Calculation of equivalent static loads

The equilibrium equation of a structure with nonlinear dynamic behavior is

$$\mathbf{M}(\mathbf{b})\ddot{\mathbf{z}}_{\mathrm{N}}(t) + \mathbf{C}(\mathbf{b})\dot{\mathbf{z}}_{\mathrm{N}}(t) + \mathbf{K}_{\mathrm{N}}(\mathbf{b},\, \mathbf{z}_{\mathrm{N}}(t))\mathbf{z}_{\mathbf{N}}(t) = \mathbf{f}(t) \tag{6}$$

where $\mathbf{M}$ is the mass matrix, $\mathbf{C}$ is the damping matrix, $\mathbf{K}_N$ is the nonlinear stiffness matrix, $\mathbf{z}_{\mathrm{N}}(t)$ is the displacement vector, $\dot{\mathbf{z}}_{\mathrm{N}}(t)$ is the velocity vector, $\ddot{\mathbf{z}}_{\mathrm{N}}(t)$ is the acceleration vector and t is the time. The subscript 'N' means that the response is obtained from nonlinear dynamic analysis. $\mathbf{f}(t)$ is the external load vector in the time domain and $\mathbf{z}_{\mathrm{N}}(t)$ at all the time steps is obtained from Eq. (6). The equivalent static loads are defined as:

$$\mathbf{f}_{\mathrm{eq}}(s) = \mathbf{K}_{\mathrm{L}}(\mathbf{b})\mathbf{z}_{\mathrm{N}}(t_s): \quad s = 1, \ldots, l \tag{7}$$

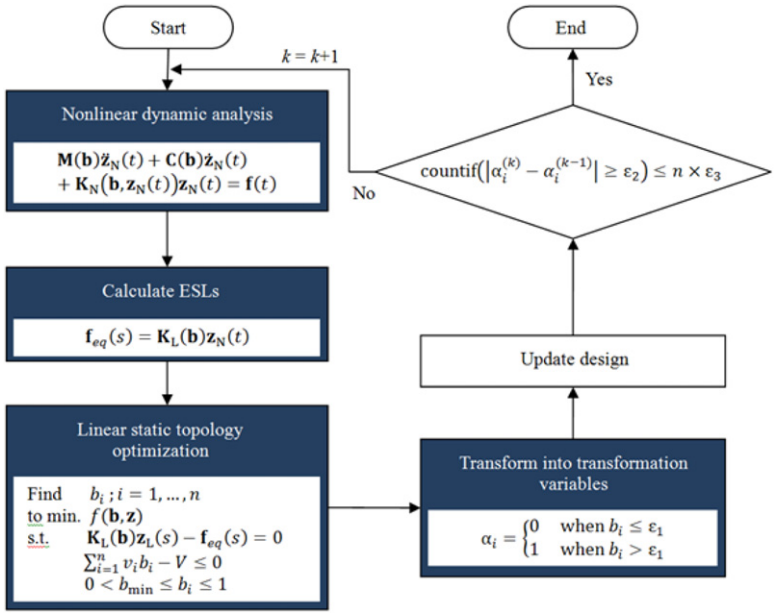

Fig. 1. Flowchart of topology optimization considering nonlinear dynamic characteristics using ESLs.

where t_s is the sth time step of the integration process of Eq. (6) and l is the total number of time steps in the time domain. The subscript 'L' means that the values are from linear static analysis. Thus, $\mathbf{K}_{\mathrm{L}}$ is the linear stiffness matrix. The ESLs vector $\mathbf{f}_{\mathrm{eq}}(s)$ is evaluated by multiplying $\mathbf{K}_{\mathrm{L}}$ and $\mathbf{z}_{\mathrm{N}}(t)$. Because $\mathbf{z}_{\mathrm{N}}(t)$ is generated from nonlinear dynamic response analysis, $\mathbf{f}_{\mathrm{eq}}(s)$ includes the inertia effect even if $\mathbf{f}_{\mathrm{eq}}(s)$ is a linear static loads set.

If the ESLs are used as external loads in linear static analysis, then the equilibrium equation is

$$\mathbf{K}_{\mathrm{L}}(\mathbf{b})\mathbf{z}_{\mathrm{L}}(s) = \mathbf{f}_{\mathrm{eq}}(s): \quad s = 1, \ldots, l. \tag{8}$$

The nodal displacement vector $\mathbf{z}_{\mathrm{L}}(s)$ in Eq. (8) has the same values as the nonlinear dynamic nodal displacement vector $\mathbf{z}_{\mathrm{N}}(t)$ in Eq. (6) at an arbitrary time t_s. The overall process of ESLSO is illustrated in Fig. 1. If the ESLs are used as external loads in linear static response topology optimization, the same displacements as the nonlinear dynamic response can be considered at the beginning of the linear static response topology optimization process.

The ESLs generate the same displacement fields in a linear static analysis and a nonlinear dynamic analysis. However, as the process proceeds in linear static response optimization, the two fields become different. Moreover, the sensitivities of the two systems are not the same. The whole procedure is cyclically repeated to compensate the differences until the convergence criteria are satisfied. This cyclic process is explained in detail in the next section. It has been validated that the differences are zeros when the process converges [21,28]. The cyclic procedure is defined as a 'cycle' and it is different from 'iteration' in linear static topology optimization.

3.2. ESLSO for nonlinear dynamic response topology optimization

The process of ESLSO for nonlinear dynamic response topology optimization consists of nonlinear dynamic analysis of Eq. (6), calculation of ESLs in Eq. (7), linear static response topology optimization, and updating the design results for nonlinear dynamic analysis of the next cycle as illustrated in Fig. 1. In linear static response topology optimization, the ith design variable b_i is the value of the artificial density between 0 and 1. After linear static response topology optimization is performed, all the elements have continuous values from zero to one. The artificial density value means the intermediate design variable for a finite element (FE). Hence the material properties of the elements are updated by the artificial density for the nonlinear FE model in the next cycle. When nonlinear dynamic analysis is carried out with the FE model which is updated according to the values of the artificial density, mesh distortion should not occur. Transformation variables and a new updating method are introduced to prevent the mesh distortion problem, and this will be explained later.

The steps of the proposed nonlinear dynamic response topology optimization process are as follows:

Step 1. Set the initial design variables and parameters (cycle number: $k = 0$, design variables: $\mathbf{b}^{(k)} = \mathbf{b}^{(0)}$, separation parameter: a certain value ε_1, convergence parameters: small numbers ε_2 and ε_3).

Step 2. Perform nonlinear dynamic analysis with $\mathbf{b}^{(k)}$ in Eq. (6).

Step 3. Check the response profile of the compliance in the nonlinear dynamic system that is $\boldsymbol{\sigma}_u^{\mathrm{T}}\boldsymbol{\varepsilon}_u,\ u = 1, \ldots, l$ in Eq. (2), and find the number of peak points in the profile. The time steps for the peaks and the number of peak points are evaluated (they can be changed at each design cycle).

Step 4. Generate ESLs using Eq. (7) at the time steps near the peaks that are obtained by using Eq. (2) in Step 3.

Step 5. Solve the linear static response topology optimization problem with ESLs as follows:

$$\text{Find} \quad \mathbf{b}^{(k)} \in R^n \tag{9a}$$

$$\text{to minimize} \quad \sum_{u=1}^{p} w_u \left(\mathbf{f}_u^{\mathrm{T}}\mathbf{z}_u\right): \quad u = 1, \ldots, p \tag{9b}$$

$$\text{subject to} \quad \mathbf{K}_{\mathrm{L}}(\mathbf{b}^{(k)})\mathbf{z}_{\mathrm{L}}(u) - \mathbf{f}_{\mathrm{eq}}(u) = 0: \quad u = 1, \ldots, p \tag{9c}$$

$$\mathbf{v}^{\mathrm{T}}\mathbf{b} \le V \tag{9d}$$

$$0.0 < b_{\min} \le b_i \le 1.0: \quad i = 1, \ldots, n. \tag{9e}$$

The summation of the compliance of the p loading conditions in Eq. (9a)(c) is considered as the objective function in Eq. (9a)(b). p is determined in Step 3.

Step 6. Transform the values of the design variables into the values of the transformation variables as follows:

$$\alpha_i = \begin{cases} 0 & \text{when } b_i \le \varepsilon_1 \\ 0 & \text{when } b_i > \varepsilon_1 \end{cases}: \quad i = 1, \ldots, n \tag{10}$$

where b_i is the ith optimum design variable obtained in Step 5. α_i is the transformation variable for b_i. The total number of the transformation variables is the same as that of the design variables. The separation parameter ε_1 is a certain value between $b_{\min}$ and 1, which is defined by the user. After the linear static response topology optimization in Step 5, most of the design variables have values close to $b_{\min}$ or 1. But some design variables may be far from $b_{\min}$ and 1. In this case, the transformation variables in Eq. (10) are exploited. If the value of a design variable is smaller than the separation parameter, the corresponding transformation variable has a value of 0. Otherwise, the corresponding transformation variable is regarded as 1. Therefore, all the transformation variables have the value of 0 or 1.

Step 7. Update the FE model for nonlinear dynamic response analysis using the transformation variables in Step 6. If α_i is 1, the corresponding finite element remains in nonlinear dynamic response analysis. Otherwise, the corresponding element is removed. Therefore, the mesh distortion problem is eliminated because the elements with small b_i in Step 5 are removed in nonlinear dynamic response analysis. If ε_1 in Eq. (10) is too small, few elements are removed and the total number of cycles might be increased. If ε_1 is large, the number of removed elements can be too many. Then the FE model, which has a much smaller volume than the specific volume defined in Eq. (1a)(d) or (9a)(d), can be made. Depending on the value of ε_1, disconnection between neighboring finite elements might occur in the updated FE model. Thus, the percentage in the volume constraint (volume fraction) of topology optimization is recommended for ε_1. However, this technique does not always work well and additional research is needed for the decision of ε_1. For example, Step 6 can be applied to the FE model that could be generated by using the post-processing or filtering technique [29] for the results of linear static response topology optimization in Step 5.

The updated FE model is utilized for nonlinear dynamic response analysis in Step 2 and calculating ESLs in Step 4. In the updated FE model, some elements do not exist due to the values of the transformation variables. If the updated FE model is utilized again in linear static response topology optimization, the eliminated elements cannot be recovered in the next cycle because the eliminated elements are not defined as design variables. Therefore, the updated FE model is not used in Step 5. Instead, the model with full finite elements is used for linear static topology optimization in Step 5.

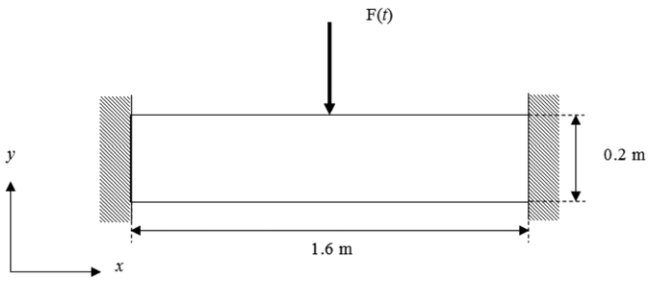

Fig. 2. Problem description of a plate fixed along both ends.

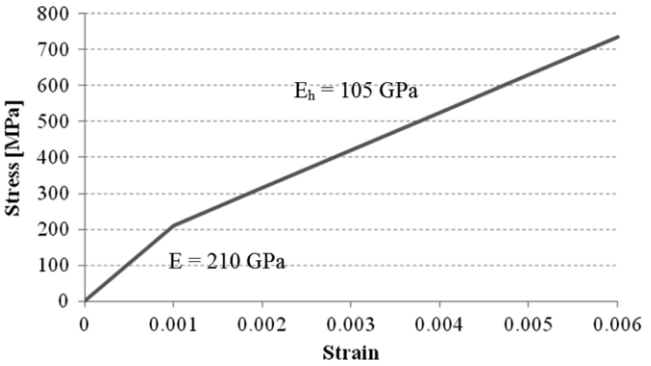

Fig. 3. Material profiles of a plate fixed along both ends.

Step 8. When $k = 0$, $k = k + 1$ and go to Step 2 for the next cycle. Otherwise, if

$$\text{countif}\left(\left|\alpha_i^{(k)} - \alpha_i^{(k-1)}\right| \geq \varepsilon_2\right) \leq n \times \varepsilon_3: \quad i = 1, \ldots, n \tag{11}$$

then terminate the process. The convergence parameter ε_2 is an arbitrary value between 0 and 1 because α_i has a value of 0 (non-existent element) or 1 (existent element). ε_3 is a certain percentage. The number of transformation variables, which are changed more than ε_2 between the adjacent cycles, is counted. If the counted number is smaller than $(n \times \varepsilon_3)$, the process terminates. Otherwise, $k = k + 1$ and go to Step 2.

4. Examples

4.1. Example 1: a plate fixed along both ends

A plate illustrated in Fig. 2 is selected. The width is 1.6 m, the length is 0.2 m and the thickness of the plate is 0.001 m. This example is used as a standard example in many studies on linear static response topology optimization [30,31]. Also, the results can be easily evaluated and compared. Fig. 3 illustrates the strain–stress curve of the used material, and the material density is 7850 kg/m^3. In the analysis, the quadrilateral fully integrated finite-membrane-strain elements are employed for the FE model and these elements allow transverse shear deformation. No spurious membrane or bending zero energy modes exist because the stiffness of the elements is fully integrated. All the shell elements use bending strain measures which are approximations to those of the Koiter–Sanders shell theory [32], and the strain method based on the Hu–Washizu principle is employed.

Fig. 4 presents the applied dynamic load profile (5 Hz). The natural frequency of the structure in Fig. 2 is 2.119 Hz. When the natural frequency is very large (the structure is stiff), a structure is affected little by dynamic external loads. If the structure has larger natural frequency than the frequency of the force, the behavior of the structure is similar to the static case [33]. However, when the natural frequency of the structure is smaller than the frequency of the force, or the natural frequency is similar to the frequency of the applied force, we should consider the dynamic effects [33]. Thus, the dynamic characteristics (inertia effect) should be considered in this example because the frequency of the force in Fig. 2 is larger than the natural frequency. Topology optimization is carried out with the initial model in

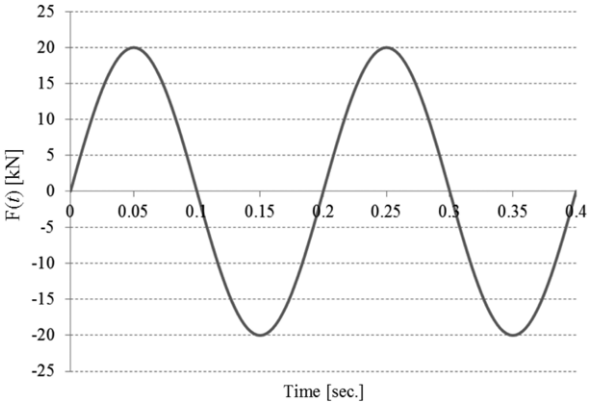

Fig. 4. Load profiles of a plate fixed along both ends.

which all the design variables corresponding to the finite elements have a value of 1. During the process of topology optimization, the natural frequency of the structure could be reduced because the mass of the structure is decreased. Therefore, although the natural frequency of the initial model and the frequency of the force are similar, the natural frequency of the structure becomes smaller and the dynamic effect is important. Designers should pay attention to the relationship between the frequency of the force and the natural frequency to justify the dynamic response topology optimization process.

The example considers geometric, material and both nonlinearities, respectively. The material properties in the elastic range in Fig. 3 are utilized for the example that only considers the geometric nonlinearity. As illustrated in Fig. 4, the maximum magnitude of the applied load is 20 kN and the total number of time steps is 4000.

The total number of the finite elements is 5000 and the number of design variables is equal to the number of elements. The objective function to be minimized is the weighted summation of the compliances near the peaks as in Eq. (9a)(b). The compliance profile of the initial FE model is checked by Eq. (2), and the number of peaks is 4. Five time steps near each peak are selected. Thus, p in Eq. (4) is 20 and this value is used for linear static response topology optimization in Eq. (9a) at the first cycle. As mentioned earlier, the number of peaks can be changed during the optimization procedure. Hence the number of peaks should be checked at each design cycle. The peaks are automatically checked by using a program developed for the automatic ESLSO process. The weighting factors w_u of Eq. (9a)(b) are set to 1.0 and the volume fraction in Eq. (9a)(d) is 30%.

The results of nonlinear dynamic response topology optimization are illustrated in Fig. 5. Fig. 5(a) demonstrates the results of linear static response topology optimization with Eq. (1a) using a commercial software system [5]. The load for linear static response topology optimization is a static load of 20 kN which is the maximum magnitude of the dynamic load. Figs. 5(b), (c) and (d) present the results of nonlinear dynamic response topology optimization using ESLs. In Figs. 5(b) and (c), member A reduces the deflection of the structure in the time domain, and member B prevents the deflection of the bottom part as well. In Fig. 5(c) where material nonlinearity is considered, the strain of the bottom part is reduced by the fact that member C supports members A and B widely. In Fig. 5(d), when the material and geometric nonlinearities are considered, the strain is very large and the tensile stress increases at the points near the center. Member D prevents the deflection of the structure, and member E and member F reduce the bending of the structure.

As shown in Table 1, the optimization process for geometric or both nonlinearities converges in 3 cycles. The number of cycles is 4 for the problem considering material nonlinearity. The number of cycles is equal to the number of nonlinear dynamic analyses. Table 2 shows the maximum strain energy of the structure when nonlinear dynamic analysis considering geometric, material or both nonlinearities is performed with the results of topology optimization in Fig. 5. Because the objective function is to minimize the peaks of the compliance, the maximum values of the compliance function are compared. When nonlinear dynamic analysis with the results is performed, the FE models in Fig. 5 are modified because the four FE models do not exactly have 30% volume. The thicknesses of the FE models are tuned so that the volumes of the four results have the same values. In Table 2, each row shows the results of topology optimization and each column shows the type of nonlinear dynamic analysis. As shown in Table 2, the results of nonlinear dynamic topology optimization using ESLs are always better than those of linear static response

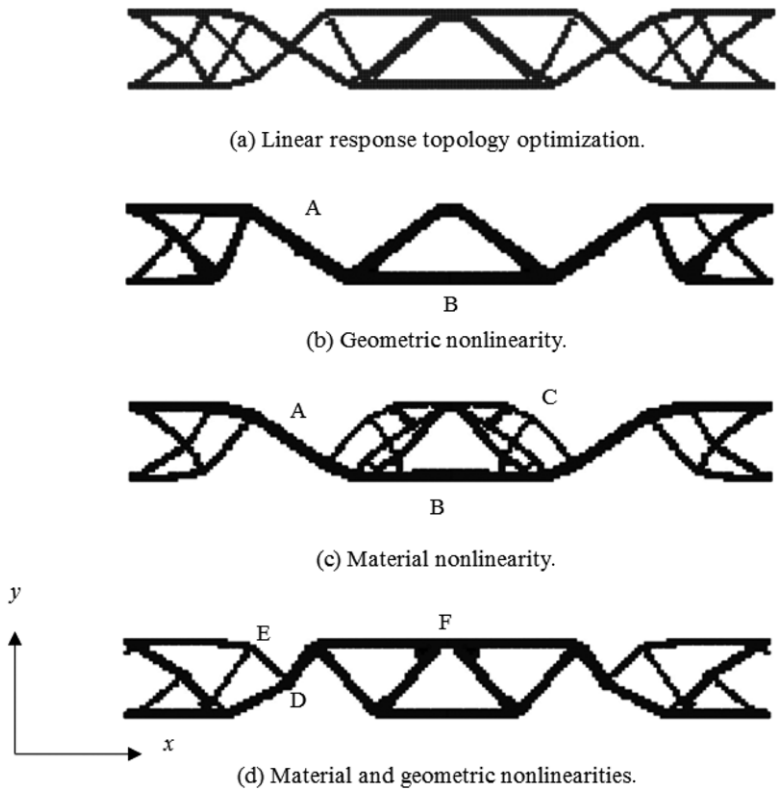

Fig. 5. Results of topology optimization considering nonlinear dynamic characteristics for a plate (the maximum magnitude of applied load = 20 kN, the forced frequency = 5 Hz).

Table 1
Optimization results for a plate fixed along both ends.

	Linear optimization	Nonlinear dynamic optimization using ESLSO		
		Considering geometric nonlinearity	Considering material nonlinearity	Considering both nonlinearities
No. of iterations	19	–	–	–
No. of cycles	–	3	4	3
No. of nonlinear dynamic analyses	–	3	4	3
Total CPU time (s)	52	3219	3852	3004

optimization. The results show that when there are nonlinear dynamic characteristics in the structure, linear static topology optimization is not sufficient.

As the second case, nonlinear static topology optimization is carried out with the structure in Fig. 2 to compare the results of nonlinear dynamic and static response topology optimization. The maximum magnitude of the applied static load is 20 kN, and geometric and material nonlinearities are considered. The second case is solved by using the method for nonlinear static response topology optimization in Ref. [18]. The results are shown in Fig. 6. Nonlinear static response topology optimization converges in 4 cycles. As illustrated in Figs. 5(a) and 6(a), the results of linear static topology optimization are the same regardless of the dynamic effects of the applied load. The results in Figs. 5(d) and 6(b) are quite different because dynamic effects are not considered in the second case. As illustrated in Figs. 5 and 6, nonlinear dynamic response topology optimization should be carried out when the dynamic effect is important. In Table 2, the results of Fig. 6(b) are analyzed by nonlinear dynamic analysis. The strain energy is improved when the dynamic effect is considered in the optimization.

Table 2
Maximum strain energy from nonlinear dynamic analysis for a plate fixed along both ends.

		Maximum strain energy from nonlinear dynamic analysis (J)		
		Considering geometric nonlinearity	Considering material nonlinearity	Considering both nonlinearities
Linear topology optimization		113.695	313.590	340.031
Nonlinear dynamic response topology optimization (the maximum magnitude of applied load = 20 kN, the frequency of the applied load = 5 Hz)	Considering geom. nonlinearity	109.149		
	Considering mat. nonlinearity		289.941	
	Considering geom. and mat. nonlinearities			309.894
Nonlinear static response topology optimization	Considering geom. and mat. nonlinearities			319.316

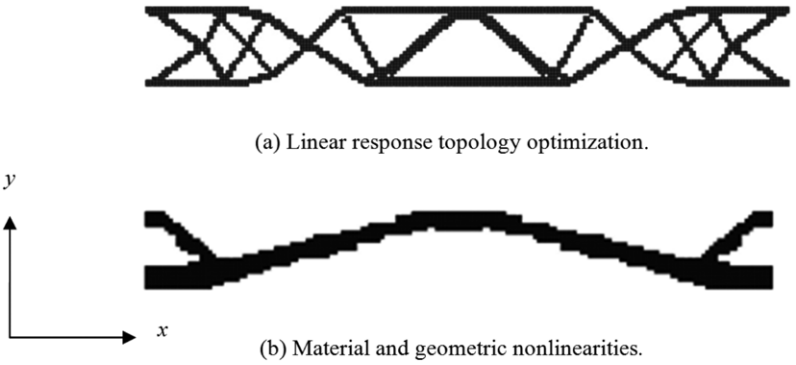

(a) Linear response topology optimization.

(b) Material and geometric nonlinearities.

Fig. 6. Results of topology optimization considering nonlinear static characteristics for a plate (the maximum magnitude of applied load = 20 kN).

For the third case, additional nonlinear dynamic response topology optimization is performed with the structure in Fig. 2. The maximum magnitude of the applied load is 10 kN and the frequency of the force is 1 Hz. Because the frequency of the force is smaller than the natural frequency of the structure, the dynamic effect can be very small in the third case. Other conditions except for the maximum magnitude and the frequency of the force are the same as those of the first case. The results of the third case are presented in Fig. 7. As illustrated in Figs. 5(a) and 7(a), the results of linear static response topology optimization are the same regardless of the applied load. It is noted that the magnitude of the load does not have any influence in linear static response topology optimization. The results in Fig. 7(b) are almost similar to the results of linear static topology optimization because the applied load does not lead nonlinearities and the occurrence of the inertia effect. The third case converges in 4 cycles. As illustrated in Fig. 7, if the dynamic effect and nonlinearity are not large, a good solution can be obtained from linear static response topology optimization. However, nonlinear dynamic topology optimization should be performed when those effects are crucial.

4.2. Example 2: a crash box for crashworthiness

Crashworthiness design is of special interest in the automotive industry and the transportation safety field. Topology optimization in crashworthiness design has been attempted by finding an efficient solution algorithm [11–13]. In the event of a crash, the impact energy transmitted to the inside of the vehicle should be reduced by the structural components that absorb energy for safety. The ultimate goal of crashworthiness optimization is to find the structure that minimizes the injuries of passengers [34]. From this viewpoint, the purpose of topology optimization in crashworthiness is to maximize the strain energy of the structure because the structure must absorb the impact energy as much as possible [13,35].

RCAR (Research Council for Automobile Repairs) is an international organization that works towards reducing insurance costs by improving automotive damageability, reparability, safety and security [36]. RCAR established a test to evaluate the performance of crashworthiness. Fig. 8 shows the RCAR test of the frontal structure of an automobile.

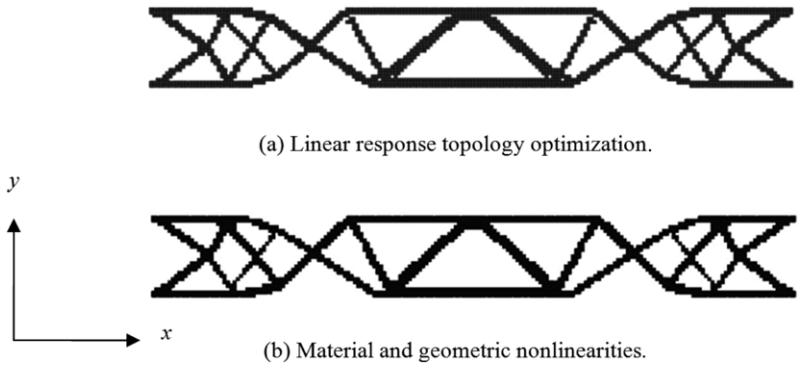

Fig. 7. Results of topology optimization considering nonlinear dynamic characteristics for a plate (the maximum magnitude of applied load = 10 kN, the forced frequency = 1 Hz).

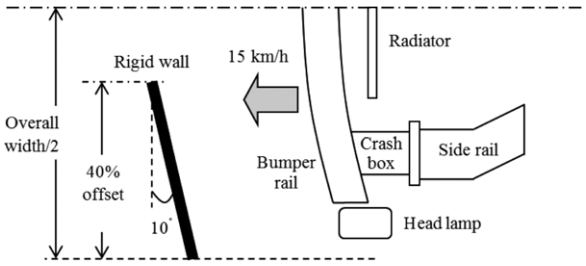

Fig. 8. RCAR test conditions for the frontal structure of the vehicle.

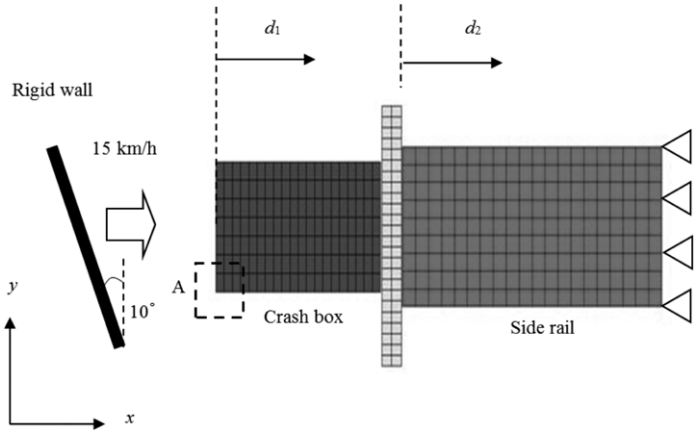

Fig. 9. Finite element model for designing the crash box.

In this test, the speed of the vehicle is 15 km/h and it has a 40% offset with a rigid barrier angled at 10°. After the first impact at the bumper rail, the residual energy which is not absorbed by the bumper rail is transmitted to the crash box and the side rail. If the crash box cannot totally absorb the residual energy, the repair cost is increased due to the damage of the side rail because the side rail is connected to the vehicle body. Therefore, the crash box must absorb the residual energy completely. The crash box is selected as an example for crashworthiness design using topology optimization.

Fig. 9 illustrates the FE model for topology optimization with the crash box. Because using the full vehicle for design is extremely expensive, a simple FE model with the side rail and the crash box is utilized. The width of the

crash box is 0.2 m, the height is 0.15 m and the length in the x direction is 0.3 m. The fully integrated eight-node hexahedron solid elements are utilized for the FE model in the analysis. Two types of steel material are used for the crash box and the side rail. There is contact nonlinearity between the crash box and the rigid wall. Geometric and material nonlinearities are considered as well.

The design domain is defined only on the crash box and the optimization formulation is as follows:

$$\text{Find} \quad b_i: \quad i = 1, \ldots, 6804 \tag{12a}$$

$$\text{to maximize} \quad \sum_{s=1}^{p} \text{strain energy}_s \tag{12b}$$

$$\text{subject to} \quad \mathbf{K}_{\mathrm{L}}(\mathbf{b}^{(k)})\mathbf{z}_{\mathrm{L}}(s) - \mathbf{f}_{\mathrm{eq}}(s) = 0: \quad s = 1, \ldots, q \tag{12c}$$

$$\sum_{i=1}^{6804} v_i b_i - V \leq 0: \quad i = 1, \ldots, 6804 \tag{12d}$$

$$d_1 \leq d_{1,\,\text{allowable}} \tag{12e}$$

$$d_2 \leq d_{2,\,\text{allowable}} \tag{12f}$$

$$0.01 < b_{\min} \leq b_i \leq 1.0: \quad i = 1, \ldots, 6804. \tag{12g}$$

The absorbed energy of the crash box is continually increased during the crash process. Therefore, the crash box may absorb the maximum energy when the impact is almost finished. The objective function is defined to maximize the strain energy of the crash box at some time steps near the end time of the impact. p in Eq. (12a)(b) denotes the number of time steps near the end time of the impact, and p is 5 in this example. The first displacement constraint in Eq. (12a)(e) is added to prevent damage to the interior components such as the radiator or head lamps in Fig. 7 because the purpose of the RCAR test is to reduce the repair cost. The crash box can maintain some stiffness due to this displacement constraint. The damage of the side rail is eliminated by the second displacement constraint in Eq. (12a)(f). V in Eq. (12a)(d) is 50% as the volume fraction. If the value of the volume fraction is too small, the finite elements may remain only at the part where the crash box and the rigid wall collide. On the other hand, if it is too large, it is difficult to determine the layout with the results of topology optimization due to many remaining finite elements. The extrusion condition in the x-direction is considered for manufacturing because the bumper rail and the side rail cannot be connected without the extrusion condition.

Fig. 10 presents the optimization results of the crash box. The optimization process converges in 7 cycles. As illustrated in Fig. 10(b), the elements in the x-direction have the same value of design variables because the extrusion condition is used. In Fig. 9, Part A is the primary contacted part when the crash box is impacted on the rigid wall. The materials remain in Part A because the crash box should maintain stiffness due to the first displacement constraint in Eq. (12a)(e). As illustrated in Fig. 10, a partition such as Part B exists in the middle of the crash box. Because Part B and the outside panels are deformed together, the absorbed energy of the crash box is increased. And the displacement constraints are satisfied by maintaining the stiffness of the structure. When there are contact conditions in the structure, linear static response topology optimization cannot be carried out because of contact nonlinearity. Thus, it is not possible to compare the results of Fig. 10 with the results of linear static topology optimization.

Fig. 11 shows the force–displacement curve (f–d curve) when the crash analysis is performed with the results of topology optimization in Fig. 10. In the f–d curve, the area under the curve means the absorbed energy. If the initial peak in the f–d curve is generated rapidly and the reaction force at the initial peak is maintained during the crash, the absorbed energy of the structure is increased because of the large area under the curve. In Fig. 11, it is shown that the initial peak of the reaction force of approximately 9.38 kN occurs when the displacement is 3.28 mm. The maximum displacement is 50 mm and the maximum reaction force is 9.49 kN when the displacement is 50 mm. If the maximum possible absorbed energy based on the maximum displacement (50 mm) and the maximum reaction force (9.49 kN) is assumed to be 100%, the area under the curve in Fig. 11 is 72.28%. The new crash box in Fig. 11 may absorb a lot of the energy, however, manufacturing the product based on the results can be expensive. If a detailed design such as size or shape optimization is performed with the topology optimization results, a reasonable design can be obtained. A design flow for such a design has been proposed [37].

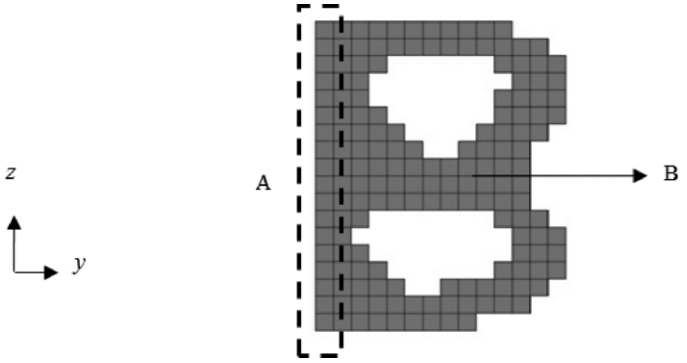

(a) Side view.

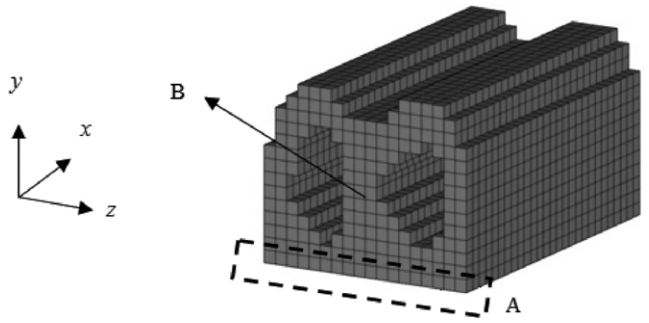

(b) Isometric view.

Fig. 10. Optimization results of the crash box.

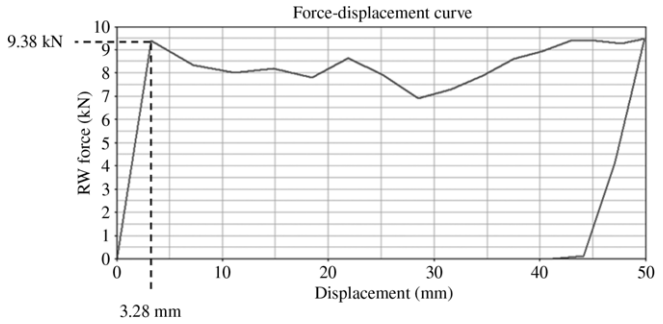

Fig. 11. The force–displacement (f–d) curve of the crash event with the results of topology optimization.

5. Conclusions

Nonlinear dynamic response topology optimization is performed using ESLSO with the transformation variables and the newly defined objective function. In ESLSO, nonlinear analysis is performed, ESLs are generated at each time step, linear static response topology optimization is carried out the ESLs and the process cyclically proceeds until the convergence criteria are satisfied. The transformation variables which correspond to the design variables are defined to overcome the mesh distortion problem that is a typical obstacle in nonlinear response topology optimization. After linear static response topology optimization, if the value of a design variable is smaller than a certain value, the corresponding transformation variable is 0. Otherwise, the corresponding transformation variable is 1. The elements for the transformation variables with zeros are eliminated in the FE model for nonlinear dynamic response analysis. The proposed objective function is to minimize the weighted summation compliance near the peak points to prevent a large deformation at a certain time. The newly proposed ESLSO is applied to two examples that are a simple plate

structure and the crash box for the crashworthiness design. The results show that the proposed method provides quite an excellent solution. It is well known that nonlinear dynamic response optimization is quite expensive for a large scale structure. The results of the examples show that the process terminates in a few cycles with ESLSO. It means that only a few nonlinear dynamic analyses are required. Additional research is needed as well. For example, a technique to determine the separation parameter for the transformation variable should be established, or various responses such as the stresses and eigenvalues should be considered in the objective function or constraints.

Acknowledgments

This work was supported by the research fund of Hanyang University (HY-2013-P). The authors thank Mrs. MiSun Park for her English correction of the manuscript.

References

[1] M.P. Bendsøe, O. Sigmund, Topology optimization by distribution of isotropic material, in: Topology Optimization: Theory, Methods and Applications, Springer, Germany, 2003, pp. 1–69.
[2] M.P. Bendsøe, N. Kikuchi, Generating optimal topologies in structural design using a homogenization method, Comput. Methods Appl. M. 71 (2) (1988) 197–224.
[3] M.P. Bendsøe, Optimal shape design as a material distribution problem, Struct. Optim. 1 (4) (1989) 193–202.
[4] MD NASTRAN R3 User's Manual, MSC Software Co., Santa Ana, CA, USA, 2008.
[5] GENESIS 10.0 User's Manual, Vanderplaats Research and Development, Inc., 2009.
[6] Altair OptiStruct, Introduction to OptiStruct FEA Version 10.0, Altair Engineering, Inc., MI, USA, 2009.
[7] K.J. Bathe, Finite Element Nonlinear Analysis in Solid and Structural Mechanics, in: Finite Element Procedures in Engineering Analysis, Prentice Hall, Englewood Cliffs, NJ, USA, 1996, pp. 485–628.
[8] J.N. Reddy, Material nonlinearities and coupled problems, in: An Introduction to Nonlinear Finite Element Analysis, Oxford University Press, NY, USA, 2004, pp. 389–395.
[9] S.J. Min, N. Kikuchi, Y.C. Park, S. Kim, S. Chang, Optimal topology design of structures under dynamic loads, Struct. Optim. 17 (1999) 208–218.
[10] H.H. Jang, H.A. Lee, G.J. Park, Preliminary study on linear dynamic response topology optimization using equivalent static loads, Trans. Korean Soc. Mech. Eng. 33 (12) (2009) 1357–1493 (in Korean).
[11] R.R. Mayer, N. Kikuchi, R.A. Scott, Applications of topology optimization techniques to structural crashworthiness, Internat. J. Numer. Methods Engrg. 39 (8) (1996) 1383–1403.
[12] J. Forsberg, L. Nilsson, Topology optimization in crashworthiness design, Struct. Multidiscip. Optim. 33 (1) (2007) 1–12.
[13] N.M. Patel, B.S. Kang, J.E. Renaud, A. Tovar, Crashworthiness design using topology optimization, J. Mech. Des. 131 (6) (2009) 061013. 1–12.
[14] G.H. Yoon, Y.S. Joung, Y.Y. Kim, Optimal layout design of three-dimensional geometrically non-linear structure using the element connectivity parameterization method, Internat. J. Numer. Methods Engrg. 69 (6) (2007) 1278–1304.
[15] G.H. Yoon, Y.Y. Kim, Topology optimization of material-nonlinear continuum structures by the element connectivity parameterization, Internat. J. Numer. Methods Engrg. 69 (10) (2007) 2196–2218.
[16] C.B.W. Pedersen, T. Buhl, O. Sigmund, Topology synthesis of large-displacement compliant mechanisms, Internat. J. Numer. Methods Engrg. 50 (12) (2001) 2683–2705.
[17] T.E. Bruns, D.A. Tortorelli, An element removal and reintroduction strategy for the topology optimization of structures and compliant mechanisms, Internat. J. Numer. Methods Engrg. 57 (10) (2003) 1413–1430.
[18] H.A. Lee, G.J. Park, Topology optimization for structures with nonlinear behavior using the equivalent static loads method, Trans. ASME, J. Mech. Des. 134 (3) (2012) 031004.
[19] W.S. Choi, G.J. Park, Structural optimization using equivalent static loads at all the time intervals, Comput. Methods Appl. Math. 191 (19–20) (2002) 2105–2122.
[20] M.K. Shin, K.J. Park, G.J. Park, Optimization of structures with nonlinear behavior using equivalent loads, Comput. Methods Appl. Math. 196 (4–6,1) (2007) 1154–1167.
[21] Y.I. Kim, G.J. Park, Nonlinear dynamic response structural optimization using equivalent static loads, Comput. Methods Appl. Math. 199 (9–12) (2010) 660–676.
[22] H.H. Jang, H.A. Lee, J.Y. Lee, G.J. Park, Dynamic response topology optimization in the time domain using equivalent static loads, AIAA J. 50 (1) (2011) 226–234.
[23] ABAQUS/Standard Version 6.8 User's Manual, SIMULIA, Providence, RI, 2008.
[24] LS-DYNA User's Manual, Livermore Software Technology Co., Livermore, CA, USA, 2006.
[25] MD NASTRAN 2006 DMAP Programmer's Guide, MSC. Software Co., Santa Ana, CA, USA, 2006.
[26] B. Stroustrup, The C++ Programming Language, Addison Wesley, USA, 2000.
[27] C.C. Hsieh, J.S. Arora, Design sensitivity analysis and optimization of dynamic response, Comput. Methods Appl. Math. 43 (2) (1984) 195–219.
[28] G.J. Park, B.S. Kang, Validation of a structural optimization algorithm transforming dynamic loads into equivalent static loads, J. Optim. Theory Appl. 118 (1) (2003) 191–200.

[29] S. Xu, Y. Cai, G. Cheng, Volume preserving nonlinear density filter based on heaviside functions, Struct. Multidiscip. Optim. 41 (4) (2010) 495–505.
[30] D.Y. Jung, H.C. Gea, Topology optimization of nonlinear structures, Finite Elem. Anal. Des. 40 (11) (2004) 1417–1427.
[31] K. Maute, E. Ramm, Adaptive topology optimization, Struct. Optim. 10 (2) (1995) 100–112.
[32] B. Budiansky, J.L. Sanders, On the Best First-Order Linear Shell Theory, in: Progress in Applied Mechanics, The Prager Anniversary Volume, Macmillan, London, 1963, pp. 129–140.
[33] H.A. Lee, Y.I. Kim, B.S. Kang, J.S. Kim, G.J. Park, An investigation of dynamic characteristics of structures subjected to dynamic load from the viewpoint of design, Trans. Korean Soc. Mech. Eng. (A) 30 (10) (2006) 1194–1201 (in Korean).
[34] M.M. Sadeghi, Evaluation and design of vehicle structures for crash protection—a systems approach, Int. J. Crashworthiness 2 (1) (1997) 55–72.
[35] K. Witowski, A. Erhart, P. Schumacher, H. Müllerschön, Topology optimization for crash, in: 12th International LS-DYNA Users Conference, June 3rd–5th 2012, Dearborn, Michigan, USA, 2012.
[36] Research Council for Automobile Repair (RCAR). http://www.rcar.org/index.htm.
[37] S.J. Lee, H.A. Lee, S.I. Yi, D.S. Kim, H.W. Yang, G.J. Park, Design flow for the crash box in a vehicle to maximize energy absorption, Proc. Inst. Mech. Eng. D 227 (2) (2013) 179–200.